Curr. Issues Mol. Biol. (2001) 3(1): 15-26.

In Situ NMR Systems

Jacqueline V. Shanks*

Dept. of Chemical Engineering, 3031 Sweeney Hall, Iowa State University, Ames, Iowa 50011-2230, USA

Abstract

In situ NMR is becoming an established technology for applications in bioprocessing and metabolic engineering. The *in situ* NMR biosensor acts as a noninvasive pH, ion, and concentration meter, with ^{31}P and ^{13}C as the two main isotopes of study. A substantial data base now exists for phosphorus and carbon spectra of bacteria and yeast. *In situ* NMR can provide many of the state variables needed for modeling glycolytic pathway function. NMR micro-reactor technology has improved significantly in the last decade. Several designs for immobilized cell reactors have been tested, and in particular, considerable gains have been made in the feasibility of studying aerobic, chemostat cultures with *in situ* NMR. Acquisition of ^{31}P spectra from cell suspensions of 3-5% v/v under controlled conditions can be made in 3 – 7 minute time resolution in several systems.

Introduction

In the last two decades, nuclear magnetic resonance (NMR) spectroscopy has been applied for noninvasive characterization of metabolic function in many different types of living systems - from humans, animals, and plants to bacterial and yeast cells. NMR applied to living systems was originally coined *in vivo* NMR. This article will use the term *in situ* NMR for NMR spectroscopy of cells and tissues. *In situ* NMR systems imply the use of a sample chamber or micro-reactor vessel to contain the living matter within the NMR spectrometer. *In vivo* NMR is reserved for NMR metabolic studies in humans and other intact multicellular organisms.

In situ NMR is especially fascinating in that several physiological and metabolic parameters may be measured simultaneously in a cell broth or fermentation media. In other words, the NMR spectrometer for this function is a noninvasive pH, ion, and concentration sensor. The potential applications of *in situ* NMR to bioprocessing and metabolic engineering are exciting, and examples are detailed elsewhere in this volume. The disadvantages of the technology, primarily in sensitivity, limit some of this potential.

What can *in situ* NMR deliver as a biosensor? Indeed, for some metabolic processes such as glycolysis, NMR can provide many of the state variables needed for modeling metabolic function. Is *in situ* NMR best suited for micro-reactors that are especially difficult to analyze by routine methods, such as immobilized cell reactors, or can chemostats be easily studied?

This review provides a framework, though not exhaustive, with which to answer these questions. Previous reviews since 1988 describe the use of NMR spectroscopy to study cellular metabolism (1), enzyme kinetics (2), and bioreactor performance (3). Most applications of *in situ* NMR are mentioned in the text of this article, except for NMR saturation-transfer measurements for enzyme kinetics (2), and some NMR measurements for redox potential, membrane structure, and concentrations of amino acids and ions. A previous review by Lundberg (1) includes all of these topics. Finally, substantial efforts in NMR micro-reactor technology have evolved in the last ten years, and several are highlighted (4-7).

NMR Experimental Constraints

NMR Properties of Nuclei

The factors that determine the suitability of an isotope for an *in situ* NMR experiment are: the spin quantum number, the natural abundance, the sensitivity, the receptivity and the type of compounds observed in the spectrum. Table 1 provides a summary of NMR properties of the most relevant isotopes for biosensor applications.

In order to perform an NMR experiment, the nucleus in question must be NMR visible, in other words, the nucleus must have a net nuclear spin. Theoretically all nuclei that have an odd mass number or an odd atomic number possess a nuclear spin. Consequently the ^{12}C isotope cannot be observed by NMR but ^{13}C, the carbon isotope of the lower natural abundance of 1.1%, can. The most commonly studied nuclei have a spin quantum number of 1/2, as the spectra from these nuclei are the easiest to analyze. The biologically relevant isotopes for spin 1/2 nuclei are ^{1}H , ^{31}P, ^{13}C, ^{15}N, and ^{19}F. Nuclei with spin quantum numbers other than 1/2 are quadruple nuclei, whose energy transitions make the interpretation of concentrations from spectral resonances more complex, but not unfeasible. Most quadruple nuclei that are relevant in biosensor applications - ^{14}N, ^{23}Na, ^{39}K, ^{35}Cl, ^{87}Rb, and ^{133}Cs - are used to measure ion concentrations, so that analyses of very few resonances are performed.

Every NMR visible isotope resonates at its characteristic frequency, the Larmor frequency, in a given magnetic field by the Eq. [1]

$$\nu_i = \gamma_i B_o \qquad [1]$$

where ν_i is the Larmor frequency of isotope i, γ_i is the magnetogyric constant of the isotope i and B_o is the field strength of the NMR magnet. In Table 1, the Larmor frequency is given for the relevant isotopes for a 11.7 Tesla superconducting magnet. An 11.7 Tesla magnet is often referred to as a 500 MHz magnet, since ^{1}H nuclei resonate at 500 MHz in an 11.7 T field. If all ^{1}H nuclei resonate only at the Larmor frequency , then the ^{1}H spectrum would not reveal much information. However, differences in chemical and/or physical environment will cause a shift in the resonance frequency. Consequently, a spectrum will consist of a spread in frequencies of a few hundred hertz

*Corresponding author. Email: jshanks@iastate.edu

TABLE 1

NMR Properties of Relevant Isotopes for Biosensor Applications *

Isotope	Spin quantum number	NMR frequency (MHz) at 11.7 T	Natural Abundance	Sensitivity ‡	Receptivity §	Applications
^{1}H	$\frac{1}{2}$	500.0	99.98	1.0	1.0	pH, redox, hemoglobin
^{31}P	$\frac{1}{2}$	202.5	100	0.066	0.066	pH, energy, P_i, Mg^{2+}, metabolites
^{13}C	$\frac{1}{2}$	125.8	1.11	0.016	1.8×10^{-4}	pH, metabolites, redox, amino acids
^{15}N	$\frac{1}{2}$	50.6	0.37	0.001	3.7×10^{-6}	pH, metabolites, amino acids
^{19}F	$\frac{1}{2}$	470.4	100	0.83	0.83	pH, Ca^{2+}, O_2 tension, protein
^{2}H	1	76.8	0.016	9.7×10^{-3}	1.4×10^{-6}	membrane structure
^{14}N	1	36.1	99.63	0.001	0.001	intracellular NO_3^-, NH_4^-, amino acids
^{23}Na	$\frac{3}{2}$	132.3	100	0.093	0.093	intra- and extracellular Na^+
^{39}K	$\frac{3}{2}$	23.4	93.1	5.1×10^{-4}	4.7×10^{-4}	intracellular K^+
^{35}Cl	$\frac{3}{2}$	49.0	75.5	4.7×10^{-3}	3.6×10^{-3}	intracellular Cl^-
^{87}Rb	$\frac{3}{2}$	164.1	27.8	0.175	4.9×10^{-2}	intracellular K^+
^{133}Cs	$\frac{7}{2}$	65.9	100	4.8×10^{-2}	4.8×10^{-2}	intracellular K^+

* Adapted from Lundberg *et al.* (1990).

‡ Sensitivity is given for an enriched sample, relative to ^{1}H at 1.0.

§ Sensitivity multiplied by the natural abundance relative to ^{1}H at 1.0.

or less, or in parts per million (ppm) of the magnetic field strength. The chemical shift in ppm is the x axis of a spectrum.

The sensitivity of a nucleus is proportional to γ^3. The sensitivity reference is ^{1}H at 1.0. The receptivity of a nucleus is the sensitivity multiplied to the natural abundance. Hence, of the spin 1/2 nuclei, ^{1}H, ^{31}P and ^{19}F are the most receptive nuclei. However, ^{31}P is the most commonly studied nucleus *in situ* since many biological phosphates can be monitored in the ^{31}P NMR spectrum. The resonance for water in the ^{1}H spectrum masks the resonances for the metabolites, which are much less concentrated than water. Removal of the water resonance by solvent suppression techniques or selectively exciting regions away from the water reference improve the quality of spectra for metabolites. Almost as receptive as ^{1}H, ^{19}F is suited for studies using fluorinated reagents to probe intracellular environments against the fluorine-free background in cells. The ^{19}F nucleus can be used to monitor intracellular Ca^{2+} concentrations, intracellular proteins, and O_2 tension.

Enrichment can enhance the sensitivity of the NMR experiment, as can be seen in Table 1 by observing the differences in the sensitivities and receptivities of ^{13}C and ^{15}N. Although more expensive than natural isotope studies, studies with labeled ^{13}C and ^{15}N compounds can be used to trace a metabolic pathway or quantify fluxes. Natural abundance ^{13}C can provide useful results, such as detecting the presence of sugars in a fermentation broth.

Sensitivity and Time Resolution

NMR is a relatively insensitive technique. With the advent of Fourier-transform NMR, several scans may be taken and summed to make the composite free-induction-decay (FID) in the time-domain, then Fourier-transformed to the resulting absorption spectrum. The signal to noise (S/N) ratio increases with the number of scans required to result in the final spectrum. The S/N ratio is related to the concentration of nuclei, C, and the number of scans, N_s, at constant magnetic field and volume of sample in the detection region, by Eq. [2]

$$\frac{S}{N} \alpha C\sqrt{N_s} \qquad [2]$$

S/N approximately increases with $B_o^{1.75}$, but this depends on a variety of factors, including probe design (8).

Because of the inherent insensitivity of NMR, the number of cells that need to be within the detection region of the radiofrequency coil is commonly many factors higher than the cell density in many cell suspension reactors. Of course, the real factor is not the cell number but the number of NMR-visible nuclei within the detection region. Practically, this means for cell-suspension systems that the number of actively metabolizing cells is critical, especially in measuring compounds present only in energized cells, such as ATP and sugar phosphates. The method of culturing the cells may be extremely important in order to measure a NMR signal, as the culture condition may affect the size of the compartment of interest. And, the sizes of compartments may vary during the growth cycle. For example, the size of vacuoles in yeast cells increase as cells enter the stationary phase. These points can be summarized in a more explicit form of Eq. [2]. The S/N ratio for a specific resonance for compound i can be expressed as:

$$\frac{S}{N} \alpha C_{i,\,comp}\, \phi \sqrt{N_s} \qquad [3]$$

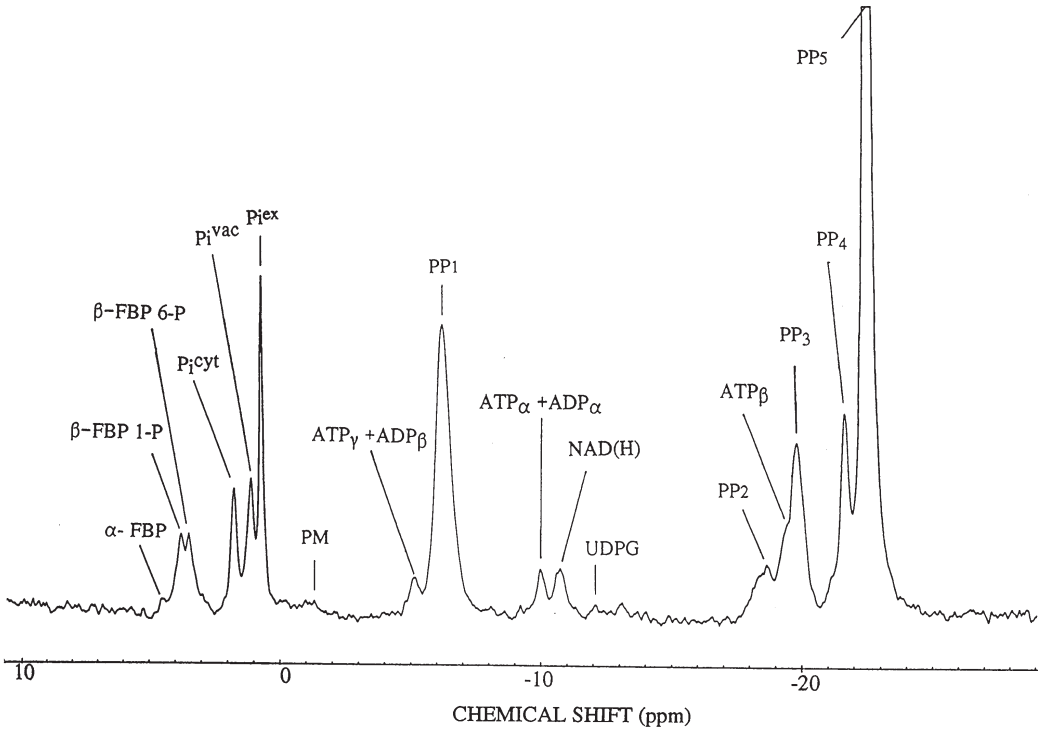

Figure 1. ^{31}P NMR spectrum at 202.46 MHz and 25°C of *S. cerevisiae* MG9A. The spectrum was taken 10 min. after addition of 75 mM glucose to a 40% (w/w) suspension of yeast cells in buffer in a 10 mm broadband probe. Accumulation time was 50 seconds. Abbreviations are: (α-FBP) a-fructose 1,6-bisphosphate; (β-FBP 1-P) 1 phosphate of β-fructose 1,6-bisphosphate; (β-FBP 6-P) 6 phosphate of β-fructose 1,6-bisphosphate; (P_i^{cyt}) cytoplasmic inorganic phosphate; (P_i^{vac}) vacuolar inorganic phosphate; (P_i^{ex}) extracellular inorganic phosphate; (PM) phosphomannan; (ATP) adenosine triphosphate; (ADP) adenosine diphosphate; (PP1) pyrophosphate and terminal phosphates of polyphosphate; [NAD(H)] nicotinamide adenine dinucleotide; (UDPG) uridinediphosphoglucose; (PP_2 and PP_3) penultimate phosphates of polyphosphate; and (PP_4 and PP_5) middle phosphates of polyphosphate.

where $C_{i,\ comp}$ is the concentration of compound i (per compartmental volume), and

$$\phi = \frac{\text{total "active" compartmental volume}}{\text{total volume of sample}} \qquad [4]$$

The time to acquire a spectrum of sufficient S/N is a limiting factor in many experiments. The time, T_a, to accumulate an FID is given in Eq. [5]:

$$T_a = T_p\, N_s \qquad [5]$$

where T_p is the pulse interval, the time between each scan. (T_p is the sum of t_p, the length of the radiofrequency pulse that excites the nuclei at the resonance condition; T_{acq}, the acquisition time; and T_{rd}, the relaxation delay). For a NMR sample consisting of a cell suspension, the approximation of T_a being inversely proportional to the square of the cell density can be seen from Eqs. [3] - [5].

A typical ^{31}P NMR spectrum for a 40 v/v% cellular suspension of *Saccharomyces cerevisiae* is shown in Figure 1. This spectrum was taken at 202.46 MHz , N_s was 120, and T_a was 1 minute. This spectrum contains resonances from the sugar phosphates; inorganic phosphate in the cytoplasm, vacuole and extracellular medium; ATP; NAD(H); and polyphosphate. A lower limit of detection in this spectrum for measuring concentrations of metabolites in the cytoplasm is approximately 0.5 mM - this concentration is based upon cytoplasmic volume ($\phi \approx 0.25$). To simply detect a resonance for 20 mM of a cytoplasmic compound, only one or two scans are needed. Figure 2 shows a ^{31}P NMR spectrum of yeast under the same experimental conditions in Figure 1 except that N_s was 2, T_a was 1.0 sec, and these cells have not been supplied with an energy source. From this ^{31}P NMR spectrum, the chemical shifts and areas of the resonances for P_i^{cyt}, P_i^{ex}, PP_1 and PP_5 can be determined. The levels of the sugar phosphates and ATP under these environmental conditions would be 3 mM and less than 0.5 mM, respectively.

A detection limit for ^{1}H is 0.01 mM in 15 min. at high field (3). To estimate the detection limit for other isotopes, simply divide 0.01 mM by the sensitivity or receptivity and by ϕ. This calculation does not take into account effects of the spin-lattice relaxation time (T_1), spin-spin relaxation time (T_2), and nuclear Overhauser enhancement (NOE) on the intensity (9). Optimal S/N ratios are obtained for spectra in which the interval between scans is less than the 4 T_1 required for complete relaxation of the nuclei before the next pulse. Multiplets, which result from spin-spin coupling of NMR-visible nuclei though bonds, can provide data on structure of a compound. However, ^{13}C-^{1}H coupling can complicate NMR spectra. Continuous ^{1}H decoupling can result in a collapse of a multiplet into one, which then

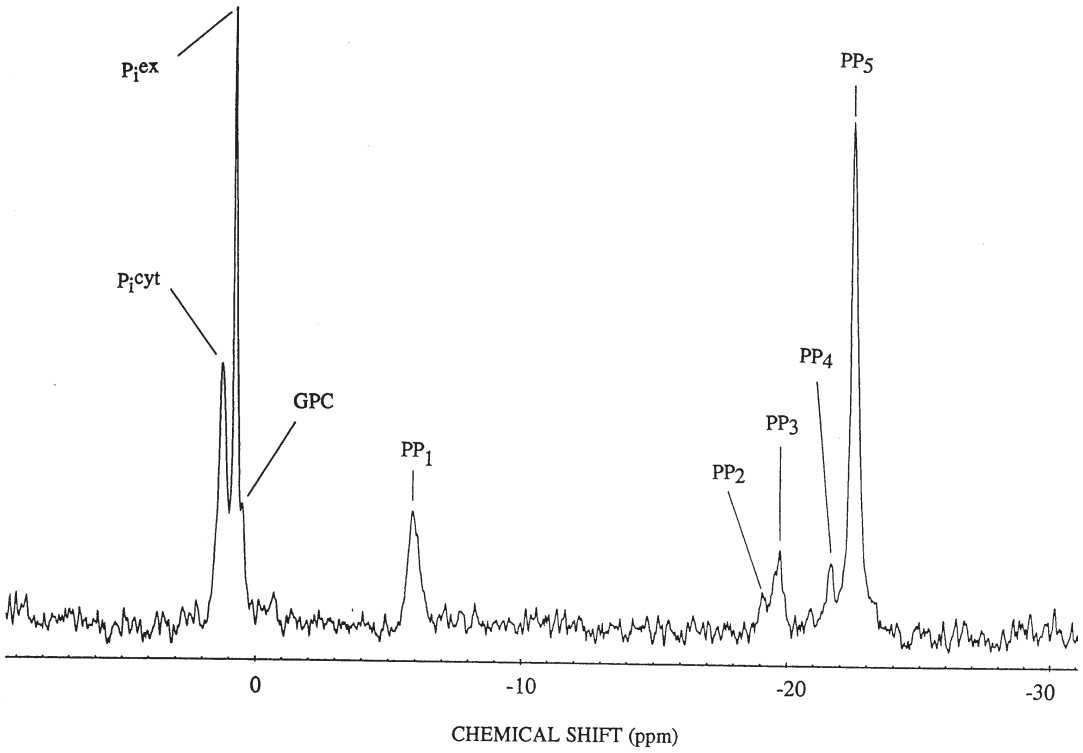

Figure 2. A one second ^{31}P NMR spectrum of resting cells of *S. cerevisiae*. The experimental conditions were the same as in Figure 1, except only two scans were taken and glucose was not added to the cells.

enhances signal intensities; and in additional enhancements of signals by the NOE effect, which in ^{13}C NMR spectra can be up to a factor of 3. T_2 effects are described below.

Resolution, Sequestration, and Cell Extracts

Good resolution is essential for accurate determination of chemical shift values and for distinguishing among resonances having neighboring chemical shift values. The linewidth of a resonance is inversely proportional to T_2. Excellent resolution requires that the nuclei be placed in homogeneous magnetic field. Resolution in *in situ* NMR experiments is especially tricky because gases and paramagnetic ions essential to growth create havoc on field homogeneity and T_2 relaxation, and since living systems in themselves are not homogeneous. For example, in yeast, the paramagnetic ion Mn^{2+} binds tightly to P_i in the vacuole, causing the linewidth of the vacuolar resonance to increase. The P_i^{vac} resonance in some cases overlaps the many resonances for the cytoplasmic phosphates.

In general, high resolution NMR can only measure signals from freely mobile molecules. Highly immobilized molecules give signals that are too broad to observe. (One way of remembering this is the rule of thumb that the linewidth of a NMR signal is proportional to the correlation time of a molecule; thus, a constricted molecule has a longer correlation time than a rapidly tumbling molecule and hence a larger linewidth). However, some large macromolecules have been able to be monitored *in situ*, such as glycogen and trehalose by ^{13}C (10), polyphosphate by ^{31}P (11) and phosphoglycerate kinase by ^{19}F (12).

A compound may be tightly bound or be constricted in its interaction with an enzyme or protein, and consequently is too immobile to be detected in an NMR spectrum. This explanation is used for the fact that inorganic phosphate or ADP in the mitochondria is not observed in the ^{31}P NMR spectrum (13). An NMR spectrum of the cell extract will reveal the previously sequestered P_i and ADP. Thus, NMR of cell extracts are commonly used to determine the total amount of a compound in a cell.

Concentrations

Relative levels can be determined within ± 10% for many metabolites in living systems and absolute concentrations can compare well with other methods. Understanding of the factors influencing the calculation of concentrations is exceedingly important in the critical assessment of concentrations obtained from NMR data. The intensity of specific resonance is proportional to the concentration of the responsible metabolite, provided that the appropriate calibrations have been made. In order to determine relative concentrations for all metabolites, corrections for differences in T_1 and NOE must be performed, i.e. correction factors must be determined for each resonance. For calculation of absolute concentrations, the volume fraction of the cellular compartment that contributes to the NMR signal and the calibration factor for the amount of intensity per mmol of nuclei must be known. A succinct critical assessment in the quantification of concentrations *in vivo* systems has been provided (14).

Biosensor Observables

pH and Transmembrane pH

NMR, fluorescent dyes, the distribution of weak acids or bases, and micro-pH electrodes are the most commonly used methods for measuring intracellular pH (15). NMR has an advantage in that it is completely noninvasive. Although NMR has been argued to be the world's most expensive pH meter, the fact that pH values of different cellular compartments can be measured simultaneously attests to the advantages of this technique; pH can be measured for the cytoplasm, and extracellular medium in many cases. Also, pH of the vacuole and peroxisomes in yeast can be determined. NMR measurement of pH is not based on the direct detection of H_3O^+ species, mainly because this species is in too low of a concentration to be detected. However, ^{31}P, ^{13}C, ^{15}N, ^{19}F or ^{1}H NMR can be used to measure pH by indirect detection of an endogenous probe compound. The probe can be any NMR-visible nucleus that is in close proximity to a protonation site in a weak acid or base. Examples of endogenous probes used are inorganic phosphate, glucose 6-phosphate, or other sugar phosphates for ^{31}P; malate, citrate, or carnosine for ^{13}C; histidine for ^{15}N; and malate, carnosine and histidine for ^{1}H (1).

The most commonly used pH probe is inorganic phosphate in ^{31}P NMR. Intracellular pH can be determined in situ by measuring the chemical shift of the intracellular inorganic phosphate peak in the *in situ* ^{31}P NMR spectrum, and then interpolating the corresponding pH from a previously established *in vitro* relationship between pH and the P_i chemical shift (16). If two peaks in the spectrum are intracellular, one for the cytoplasm and one for the vacuole, each resonance will determine the pH of that compartment.

The pH measurement is based on the equilibrium between the two ionic species of inorganic phosphate, HPO_4^{2-} and $H_2PO_4^-$, with the H_3O^+ species:

$$H_3O^+ + HPO_4^{2-} \leftrightarrow H_2PO_4^- \qquad [6]$$

The equilibrium constant, K_1, for Eq. (6) is defined in Eq. (7) as

$$K_1 = \frac{(H_3O^+)(HPO_4^{2-})}{(H_2PO_4^-)} \qquad [7]$$

where the parentheses denote activities. In solution, the two ionic species of inorganic phosphate interconvert rapidly (about 10^9 - 10^{10} s^{-1}), and consequently are in fast exchange on the NMR timescale, so that a single resonance will be observed for inorganic phosphate according to Eq. [8]

$$\nu_{p_i} = \frac{[HPO_4^{2-}]\nu_{HPO_4^{2-}} + [H_2PO_4^-]\nu_{H_2PO_4^-}}{[P_i]} \qquad [8]$$

where ν_j is the resonance frequency for species j. When activities can be equated with concentrations in Eq. [7], substitution of Eq. [7] into Eq. [8] and rearranging yields Eq. [9]:

$$[H_3O^+] = K_1 \left(\frac{\nu_{p_i} - \nu_{HPO_4^{2-}}}{\nu_{H_2PO_4^-} - \nu_{p_i}} \right) \qquad [9]$$

In an NMR experiment, all frequencies are reported in a dimensionless frequency, the chemical shift, δ. The chemical shift value for compound S, δ_S, is defined as in Eq [10]

$$\delta_s = \frac{\nu_S - \nu_R}{\nu_R} \times 10^6 \qquad [10]$$

where R is the reference compound. The relationship between the chemical shift of the probe resonance and pH can be written by substitution of the Eq. [10] into Eq. [9] and taking the logarithm of both sides of the equation to result in Eq. [11]:

$$pH = pK_1 + \log \left(\frac{\delta_{p_i} - \delta_{HPO_4^{2-}}}{\delta_{H_2PO_4^-} - \delta_{p_i}} \right) \qquad [11]$$

Ideally, the *in vitro* solution used for the calibration must mimic the intracellular ionic strength, free Mg^{2+} level, concentrations of proteins, organic acids, etc. since these factors influence the pK_a and the binding of P_i. The ionic strength and magnesium concentration are the two most important factors in the *in vitro* calibration (16). (Constant temperature is implied). The interaction of proteins,

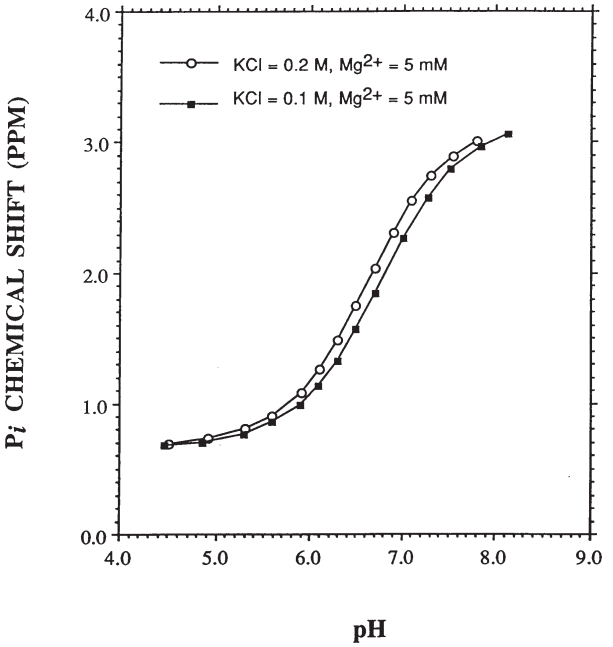

Figure 3. P_i chemical shift as a function of solution pH. Symbols show (B) 0.1 M KCl and 5 mM $MgCl_2$ and (E) 0.2 M KCl and 5 mM $MgCl_2$. The pH dependence of the chemical shift of inorganic phosphate in ^{31}P NMR is the most common method for estimation of intracellular pH. Ionic concentrations between 0.1 M and 0.2 M bracket the intracellular environment for many biological systems. From these curves it can be shown the difference in accuracy and precision of pH estimates.

mitochondria and other macromolecules with P_i can be neglected for measurement of the cytoplasmic pH (16). Figure 3 shows the pH-P_i chemical shift correlations for two solutions, one at 0.2 M KCl and 5 mM $MgCl_2$ and the other at 0.1M KCl and 5 mM $MgCl_2$.

As seen from the correlations in Figure 3, the most accurate determination of pH are for pH values within ± 1 pH unit near the pK_a values since the slope of the curves are steep in this range. In the wings of the correlation curves, a small error in the measured chemical shift can give quite a large difference in the estimated pH value. The measurement errors in the determination of chemical shifts are ± 0.02 ppm for a narrow peak, such as that for cytoplasmic inorganic phosphate in Figure 1, and up to ± 0.1 ppm for a wider peak, such as that for the terminal phosphates of polyphosphate. The error in the precision of NMR pH measurement is ± 0.02 pH units near the pK_a for a measurement error in chemical shift of ± 0.02 ppm. For minimization of the absolute error in the pH estimate, the correlation curves should bracket the true correlation curve that mimics the intracellular milieu. From Figure 3 it can be seen that if the true correlation curve is enclosed within the correlations given for 0.1 M KCl and 0.2 M KCl, then for pH values near the pK_a the error is ± 0.07 pH units. These last statements are valid given that the chemical shift reference mentioned in Eq. (6) is strictly calibrated for the *in vitro* solution and the *in situ* sample. In particular, any differences in bulk susceptibility between the calibration sample and the *in situ* sample will shift the correlation curve vertically by a constant.

The use of more than one pH indicator increases the accuracy of the pH determination, in that it provides another estimate. However, the errors associated with uncertainty in the chemical makeup of the compartmental pool are the same since the *in vitro* calibration solution used for each probe will have the same ionic strength, etc.

Alternatively, an *in situ* map of chemical shifts of two or more probes can be compared to an *in vitro* map. For example the use of inorganic phosphate and the sugar phosphates can be used to provide a more accurate estimate of cytoplasmic pH. The *in situ* chemical shift coordinates of cytoplasmic inorganic phosphate and sugar phosphates can be mapped as was done for *Saccharomyces cerevisiae* (17).

Transmembrane Concentrations and Fluxes of Ions

Concentrations of a compound in different compartments can be measured if the pH values or the ionic strength of these compartments are different, or alternatively if one compartment is exposed to a chemical shift reagent i.e. a compound that causes the chemical shift of the compound in that compartment to appear in a different chemical shift position. Thus, transmembrane fluxes of pH, inorganic phosphate, sodium, potassium and calcium can be determined in some biological systems. Inorganic phosphate resonances from the cytoplasm, vacuole, peroxisomes, and extracellular medium have been detected in the ^{31}P NMR spectrum.

Intracellular Ca^{2+} concentration is measured indirectly by using a ^{19}F-labeled Ca^{2+} chelator and recording a single ^{19}F NMR spectrum. The most commonly used chelators are fluorinated analogs of the chelator 1, 2-bis(2-aminophenoxy)ethane-tetraacetic acid (BAPTA), namely 5FBAPTA (5,5'-F-BAPTA) and 4FBAPTA (4,4'-F-BAPTA) (18, 19). The reasons for the selectivity of the BAPTA analogs for Ca^{2+} rather than Mg^{2+}, Fe^{2+} or Zn^{2+} are two fold. First, although intracellular concentrations of free Mg^{2+} ions are a thousand higher than that for Ca^{2+}, Mg^{2+} binds very weakly to the chelators. Second, even though Fe^{2+} and Zn^{2+} have higher affinities than Ca^{2+} for BAPTA analogs, the intracellular concentrations of these ions are usually very low. The accessible ranges of intracellular [Ca^{2+}] are 100 nM - 10 μM for 5FBAPTA and 300 nM - 30 μM for 4FBAPTA (19).

Nitrate and ammonium ions can be detected by both ^{14}N NMR and ^{15}N NMR spectroscopy (1, 20, 21). Although ^{14}N is a quadruple nuclei, large linewidths for nitrate and ammonium are not observed since these molecules have a high degree of symmetry (21).

The spin 3/2 nuclei - ^{23}Na, ^{39}K, ^{35}Cl, ^{87}Rb, ^{133}Cs - can be used to measure concentrations of sodium, potassium, and chlorine. The measurement of intracellular [Na^+] by ^{23}Na NMR and [K^+] by ^{39}K NMR requires the use of a chemical shift reagent to separate intracellular and extracellular resonances. The visibility of intracellular Na^+ resonance is 40% while that of the extracellular resonance is 100%. Intracellular sodium has been measured in yeast (22) and bacteria (23).

ATP, ADP, and AMP Levels

ATP, ADP, and AMP concentrations are determined using ^{31}P NMR. ATP concentrations are estimated most often by the intensity of the β-ATP resonance in the ^{31}P NMR spectrum. For yeast, the β-ATP peak is often obscured by polyphosphate resonances, as shown in Figure 1. In this case the g-ATP resonance is used, assuming that free ADP levels are very low (11).

In situ concentrations of ADP and AMP are more difficult to ascertain, and less reliable than measurements of ATP. ADP concentrations can be calculated from the difference in the area for the β-ATP resonance from the area of the γ-ATP resonance, resulting in the peak intensity of the β-ADP resonance. Polyphosphate, pyrophosphate, and tripolyphosphate resonances in the spectrum for yeast do not allow an determination of ADP concentrations by this method; use of a vacuolar mutant still produced the same result since substantial amounts of pyrophosphate and tripolyphosphate were still present (24). In most other systems the levels of ADP are so low that measurement of an area by subtraction of the two ATP resonances is not significant (1).

ADP concentrations can be estimated by a second method that uses creatine kinase. In mammalian cells with creatine kinase, the free cytosolic ADP concentration is determined by measuring the concentrations of the substrates of creatine kinase and by assuming that the reaction catalyzed by this enzyme is in equilibrium. The intracellular pH, and concentrations of ATP, phosphocreatine, free Mg^{2+} (from the chemical shift of β-ATP resonance) are determined from the *in situ* ^{31}P NMR spectrum. The creatine concentration is calculated by subtraction of phosphocreatine from the total extracted creatine levels; an equilibrium constant for the reaction must be assumed. Use of the creatine-kinase method has been extended to yeast that have been genetically modified to express rabbit muscle

creatine kinase – the ADP/ATP ratio determined by this method was approximately 2 (24). The AMP concentration can be estimated by a similar method to ADP and the creatine kinase reaction. In this case the adenylate kinase reaction is assumed to be in equilibrium; ATP and ADP concentrations are previously determined and the equilibrium constant assumed.

Carbon Metabolites

Fermentation Substrates and Products

Quantification of glucose, fructose, sucrose, ethanol, lactate, glycerol, etc. can be done with natural abundance ^{13}C NMR (25), enriched ^{13}C NMR (25-27) and ^{1}H NMR (28). This quantification includes both intracellular and extracellular levels, which can be determined separately by measurements of the medium and of the biomass (25, 27). The fate of a particular ^{13}C enriched substrate is useful to label metabolic pathways, especially for systems in which the metabolic pathways are not elucidated completely.

Concentrations of the different anomeric forms and tautomers of sugars can be determined from NMR. In natural abundance ^{13}C NMR spectra, the signals for sucrose, glucose, and fructose at common media levels can be detected. The resonances for the α and β anomers of the C-1 carbon of glucose are detected at 92.8 and 96.7 ppm, respectively. The resonances for fructose near 82 ppm indicate 5-ring tautomers of fructose and the resonance at 99 ppm indicates the 6-ring tautomers of fructose. Specific consumption rates of the α and β anomers of glucose can be determined easily from [1-^{13}C] labeled glucose, for example as was done in NMR experiments of yeast (26).

While HPLC and enzymatic assays can be used to determine concentrations of sugars and alcohols in the extracellular medium easily, NMR measurements can alleviate laborious procedures for quantification of these compounds in a transient experiment. Like HPLC, several compounds can be monitored at once with NMR; in contrast, consumption of labeled substrates can be determined in NMR experiments for systems such as yeast, on a short time scale of the order of a minute or less (10).

Quantification of intracellular products, such as glycogen and trehalose in yeast, is also feasible with NMR (26, 29). Microbial biopolymers can also be studied.

Glycolytic Intermediates

The sugar phosphates can be monitored by ^{31}P NMR or if a labeled compound is fed to the cells, by ^{13}C NMR. In comparison to ^{13}C, ^{31}P is more sensitive, better time resolution is obtained, other important variables are obtained from the same ^{31}P NMR spectrum, and the experiments are less expensive. However, the resonances of the individual sugar phosphates overlap in the ^{31}P NMR spectrum. Perchloric cell extracts (30) or deconvolution of the sugar phosphate region can be used to determine concentrations of individual sugar phosphates such as glucose 6-phosphate, fructose 1,6-bisphosphate, fructose 6-phosphate, and 3-phosphoglycerate (17). This latter technique has been used to analyze ^{13}P NMR spectra of *S. cerevisiae* (26, 29, 31) and *E. coli* (32).

Flux Measurements

The use of ^{13}C labeling and quantification of flux rates is becoming more commonplace, especially when obtained from cell extracts from microorganisms. Some of these techniques can be applied using *in situ* spectra. For example, by feeding [1-^{13}C] and [6-^{13}C] labeled glucose to yeast and analyzing the relative labels of the C1 and C6 positions of fructose 1, 6-bisphosphate, the steady-state unidirectional fluxes through the enzymes adolase and triosephosphate isomerase were obtained, and shown to operate in near equilibrium (10). The relative fluxes of competing pathways into the tricarboxylic acid cycle (TCA) cycle have been monitored, for example, in microbacterium (33), *E. coli* (34), and *S. cerevisiae* (35).

Novel Sensor Ideas

Oxygen tension can be measured indirectly by a perfluorocarbon probe and ^{19}F NMR. O_2 tension can be estimated by measuring the relaxation times of the fluorine atoms in the perfluorocarbon emulsions, since the relaxation times of these atoms are sensitive to the concentration of dissolved O_2 (36,37).

The feasibility of monitoring a fluorine-labeled enzyme *in situ* was demonstrated in yeast (12). Incubation of yeast cells with 5-fluorotryptophan resulted in the production of fluorine-labeled phosphoglycerate kinase. Specifically, two resonances were observed from two tryptophan residues in the enzyme, and an accumulation time of 9 hours was required for one ^{19}F spectrum. Although the chemical shifts of the fluorine resonances were sensitive to intracellular conditions, further research is needed for the possibility of studying specific enzyme-substrate and protein-protein interactions *in situ*.

Spectrometer Considerations in Biosensor Configuration and Operation

Magnets

The configuration of the superconducting magnet is the first consideration in designing the systems in which to use the NMR. Coupled with this factor is the expense of the magnet. Many magnets are part of a multiuser facility, and consequently any modifications to a system must be designed in consideration for the other users.

Magnet technology is continually improving. 750 MHz magnets are not uncommon and 500 MHz magnets are standard at many university NMR centers. The magnetic field strength that is optimal for one nuclei may not be the same for another, as the effects of chemical exchange and of chemical shift anisotropy lower the advantage of having a stronger field. Some *in situ* ^{31}P NMR resonances suffer from chemical shift anisotropy (13). ^{13}C NMR studies can be more advantageous at a higher field. A common compromise for sensitivity and resolution for ^{31}P and ^{13}C NMR is a 400 MHz magnet.

The strong magnetic fields that are generated by a superconducting magnet require that the reactor equipment be placed sufficiently far enough from the magnet for reasons of safety and resolution. Lines of constant magnetic field strength (gauss lines) that surround the magnet are ellipsoidal, with the major axis along the direction of the bore. For instance, for a narrow-bore 500

MHz magnet (vertical bore), return to the earth's magnetic field strength occurs at 6 m from the center of the magnet in the radial direction and 7.5 m in the axial direction. A magnet can be modified for a perfusion reservoir inside the magnet, by replacing the stack (that holds the probe) with the perfusion apparatus. While this has the advantage of shortening the flow lines, removing the stack exposes the shim coils (that adjust field homogeneity) to dust and, if the reservoir leaks, to liquid.

A wide-bore, vertical magnet with a bore size of 9 cm can hold sample sizes up to 20 mm diameter in a standard 20 mm probe. The bore of a vertical, narrow-bore magnet is 5 cm and the largest sample size in this magnet is usually a 10 mm diameter in a standard 10 mm probe. However, a narrow-bore magnet can accommodate a 15 mm or 18 mm probe, but with some loss in resolution due to the detection region extending beyond the most homogeneous part of the magnetic field. Many horizontal-bore magnets have wide bores, as in the case of imaging magnets, and can accommodate small animals and bioreactors more easily. However, the placement of fluid lines, pumps and controls must be placed farther away from this type of magnet since the radial gauss lines extend further for the horizontal magnet than for the vertical one.

Probes

The types of probes used for high field magnets include broadband, fixed-frequency, dual and quad probes. Microimaging attachments for magnets are also available. Broadband probes can be set to a specific observe isotope and perform proton decoupling. Fixed-frequency or a dedicated probe can only be used for the observe nucleus for which it was designed but has improved sensitivity over a broadband probe. The standard probe configurations holds 10mm diameter tubes for a narrow-bore magnet and 20 mm diameter tubes for a wide-bore magnet. Many *in situ* reactors are based on simple modification to the sample tube configuration. The probe configuration can be more radically altered by placing the radiofrequency coil inside a micro-reactor (4) and although the sensitivity is improved, the resolution suffers (7).

Multinuclei probes for *in situ* work include ^{31}P-^{13}C {^{1}H}, ^{23} Na- ^{31}P{^{1}H}, and ^{31}P-^{13}C- ^{15}N {^{1}H} probes. These probes offer the alternative of observing two or more nuclei almost simultaneously by accumulation of alternate scans. Since each scan lasts a few seconds or less, the observation of all the nuclei is essentially simultaneous. Alternatively, a spectrum of one nuclei can be acquired, then a spectrum of the other nuclei can be taken. A loss in the signal-to-noise ratio compared to fixed-frequency or broadband probes is one disadvantage of the multinuclear probes. However, the signal-to-noise ratio can be comparable if the sample size is increased; for example, in a 500 MHz magnet, our 15 mm ^{31}P-^{13}C {^{1}H} probe had higher signal-to-noise ratios for each nuclei than the ratios obtained from the corresponding 10 mm broadband probe (Shanks, unpublished results).

Biosensor Operation and Information

The intrinsic kinetics of cells, transport of nutrients between cells and the mass-transfer characteristics within a reactor would ideally be known for bioreactor operation. NMR can provide some of the variables for intrinsic kinetics, provided that the transport characteristics within the NMR experimental configuration are defined. This last point has not been explored in detail previously by spectroscopists using *in situ* NMR, but examination of the literature reveals different aspects of this point, and will be summarized in this section. Hence, the NMR biosensor will be classified either as a bioassay or as a microreactor. The differences between these two configurations will become evident not only in the NMR experimental configuration, but in the interpretation of the NMR results.

Bioassay

In the simplest type of NMR experiment, a sample from a fermentor or batch culture can be removed, and if the sample has sufficient cell density, an NMR spectrum could be taken immediately. Theoretically, this could be done with a sample taken at stationary phase in microbial cell culture, a sample from a fed-batch fermentation that achieves high cell densities, or with a sample of beads with entrapped cells removed from an immobilized cell reactor. Based upon Eqs. [3] and [5], for *S. cerevisiae* sample taken at stationary phase of growth, with a biomass concentration of approximately 5 g/l (dry weight), about 4 hours would be required to obtain a ^{31}P NMR spectrum with a S/N ratio of Figure 1. Consequently, most cellular samples are concentrated prior to an NMR experiment.

For cellular suspensions, centrifugation steps are necessary in order to achieve high cell densities. The sample is prepared in a given metabolic state, namely one of starvation and anaerobic conditions. The bioassay is then an assay of the cells as a functioning system, with the enzymes, ions, enzyme inhibitors, and enzyme activators present. After the sample is allowed to warm up to the desired temperature in the NMR magnet, an initial spectrum is taken, then a metabolic stimulus is added, and the experiment is followed in time. For yeast and bacteria, if the experiment is relatively short, on the order of a half hour to hour, negligible settling occurs. This requires that a mock sample is used for spectrometer setup and the real sample is used only for the experiment; alternatively, gases can be bubbled though the cell suspension for mixing and to change to aerobic conditions within the NMR.

True aerobic conditions, however, require additional restrictions on the number of cells in an NMR experiment. For example for non-growing *E. coli* cells, the maximum concentration of cells within the NMR tube for aerobic conditions without oxygen mass-transfer limitations is approximately 40 g/l (dry weight) (38), or approximately 20% v/v. Change the metabolic state from non-growth to actively respiring under growth, and one can only use 1.4 g/l (dry weight) for the bioassays under aerobic conditions.

In the case of dense yeast suspensions (40% v/v) under anaerobic conditions, only one minute is needed in order to obtain all of the concentrations of all the resonances in the ^{31}P NMR spectrum (17) as in Figure 1, and in the ^{13}C NMR spectrum (39). To quantify the ΔpH across the yeast cell membrane from the P_i^{cyt} and P_i^{ex} resonances, only 1 second is needed, as shown in Figure 2. A NMR bioassay using ^{13}C NMR on samples of the methylotrophic yeast *Hansenula polymorpha* from a

fermentor were used to trace carbon metabolism (40) and were much less expensive than ^{14}C radioactive assays. The relatively easy manner to perform a transient metabolic experiment is one of the strengths of the NMR bioassay.

What information does the bioassay give, relative to the metabolic state in the fermentor? Results from NMR bioassays has been compared to fermentor or shake flask results for *S. cerevisiae* and *E. coli.* When analyzing three recombinant yeast strains that had been altered in the glucose-phosphorylation step, the relative trends in ethanol yields in fermentation data was the same as the trends observed in the ^{13}C NMR experiments (26). The yields were higher in the NMR experiment, since the NMR experiment is performed under non-growth conditions in contrast to the batch fermentation. The fermentations and NMR experiments were performed under relatively high levels of glucose (2 wt %). The fermentations occurred within shake flasks, so oxygenation was not strictly controlled, and the NMR bioassays were performed without oxygenation. Even though the NMR bioassay was anaerobic, it did provide a representation of the cells' kinetic properties. This point is made clearer by the next study described.

E. coli that were grown in complex medium under anaerobic and aerobic conditions in a fermentor were studied using a NMR bioassay under anaerobic conditions, using glucose as the stimulus (41). Their results indicated that the NMR bioassay can be viewed as a stimulus-response experiment in order to study the properties of cells, from either anaerobic or aerobic conditions in the fermentor. 2-D gel electrophoresis from mock NMR samples confirmed proteins expected to be present under the anaerobic and aerobic conditions from the respective samples. The differences in turnover rates for ATP and NAD(H) and in intracellular pH acidification (obtained from the ^{31}P NMR spectrum) between the aerobic and anaerobic samples correlated with differences in glucose uptake and acid accumulation (41).

So although the NMR bioassay is performed under anaerobic conditions, the bioassay can measure and quantify differences in samples that were grown anaerobically versus aerobically, or between different strains cultured under the same metabolic conditions. The metabolic behavior of cells under aerobic conditions in fermentors and in bioassays under aerobic conditions to date have not been compared.

Bioreactors

The design goals for a NMR micro-reactor are the same as for a larger bioreactor in that aeration, sufficient mixing, and removal of toxic products should be met. Low sensitivity of the technique makes these design goals challenging. Some of the limitations in the NMR bioreactor design are distinct to micro-engineering and the configuration of the spectrometer. However, oxygen diffusion problems inherent in hollow fibers are also observed in NMR hollow fiber reactors, and consequently NMR involves a natural way in which to study immobilized cell reactors in particular. Fluid flow within the NMR reactor can shorten acquisition times by sweeping nuclei out of the radiofrequency coil. This phenomena contributes to the feasibility of continuous-flow reactors. Impressively, a chemostat reactor for the NMR have been constructed so that cells in a given growth state can be studied (4,7). Simpler batch reactor designs are also available. NMR reactors for cells can be categorized into four types: hollow fiber/membrane reactors, gel-immobilized cell reactors , the batch air-lift reactor, and continuous flow/chemostat reactors.

Hollow-Fiber/Membrane Reactors

Hollow fibers and membrane reactors can either be run as a diffusionally supplied reactor or convectively supplied reactor. Hollow fibers reactors for use in NMR experiments are commonly employed with cells confined in the shell side of the reactor and with nutrients being supplied by diffusion through the fiber wall (42-48). Membrane reactors can be diffusionally supplied (27,45) or convectively supplied (47), with more severe mass-transfer restrictions in the diffusionally supplied membrane reactor.

In a diffusionally supplied reactor, cells not in the proximity of the nutrient source may experience mass-transfer limitations. The thickness of the growing region can be estimated by a reaction-diffusion model. A reaction-diffusion model was formulated for *E. coli* cells grown anaerobically with glucose as the limiting nutrient in a hollow fiber reactor (43,47). ^{31}P NMR results illustrate the concepts from this model quite elegantly. At 37 °C, the actively growing region estimated by the model is a relatively small fraction of the shell volume - only 34%. A cytoplasmic pH value of 5.5 (rather than the value of 7.2 observed for healthy *E. coli* cells) and very small ATP values are observed from the ^{31}P NMR spectrum (42, 47). Since the NMR spectrometer only detects spatial averages, and as the reactor volume is filled with cells, the conclusion is that most of the cellular aggregate is not able to maintain normal physiological conditions. A lower operating temperature would repress growth such that the model estimates an effectiveness factor of 1 or in other words, growing cells occupying the entire shell side of the reactor. ^{31}P NMR spectra of *E .coli* cultured at 16 °C indicate a cytoplasmic pH of 7.0 and high levels of the sugar phosphates and ATP, thus in agreement with the model estimate (47). Since kinetic parameters used in the model were determined from experiments of cell suspension culture, one conclusion is that in this case, the metabolic behavior of immobilized cells is not intrinsically different from that of cells in suspension culture (47). In other words, changes in the local environment in terms of nutrients and products may cause the differences in metabolic behavior observed between immobilized cells and cell suspensions in this system.

Gel-Immobilized Reactors

Cells can be immobilized in gels such as agarose, calcium alginate and carrageenan. Most NMR studies have been of cells immobilized in agarose. Many researchers have immobilized cells in an agarose matrix, have measured the oxygen consumption rates, reported these oxygen consumption rates are comparable to those obtained in cell suspensions, and then suggested that the cells in this immobilized matrix have the same metabolic activity as suspended cells. Claims that cells in agarose are the same metabolically as suspended cells need to be verified.

Clearly, cells are able to be metabolically active when

immobilized in agarose in NMR reactors (49). For glucose metabolism, an oxygen consumption rate of 0.8 μmol/s was reported for *S. cerevisiae* entrapped in agarose threads and perfused in a NMR reactor (50). An oxygen consumption rate of 2 μmol/s was measured for aerobic growth of *S. cerevisiae* cells on glucose in a fermentor (51). Comparison of these two results does not necessarily mean that sufficient oxygen was not provided during the NMR perfusion experiment - measurement of mass transfer properties of the reactor would need to be determined for that conclusion. An oxygen consumption rate of 0.8 μmol/s for non-growing yeast is very plausible. Respiration may have been inhibited by other factors.

Several NMR studies of yeast immobilized in calcium alginate have been reported. In anaerobic studies, immobilization of *S. cerevisiae* cells in calcium alginate enhances ethanol productivity (ethanol per cell) over the cell suspension case (29, 52, 53) and in particular, the glucose consumption rate is increased (31, 53). Immobilized cells had more glucose-6-phosphate and less fructose-1,6-bisphosphate than suspended cells, as determined from ^{31}P NMR spectra. A kinetic model indicated that the distribution of flux control in the glucose to ethanol pathway was altered upon immobilization (31) and increased membrane permeability was hypothesized for the increase in glucose uptake rates (53). Calculation of the observable intraparticle diffusion-reaction modulus and the internal and external mass transport ratio indicated the absence of both internal and external mass transport limitations in these kinetic measurements (29, 52). Differences in cellular physiology in gel-immobilized cells versus cell suspensions may be dependent on the type of gel, the biological species, and the reactor configuration and operation.

Air-Lift Reactors

An airlift probe or a reactor with capillaries for bubbling are two ways in which to aerate cellular suspensions. Kramer and Bailey (38) measured the mass transfer coefficient, $k_l a$, for a previous design of an airlift probe (54). A maximum concentration of non-growing *E. coli* cells in a NMR cell suspension was calculated to be 41.1 g/l (20% v/v) in order to maintain aerobic conditions throughout the experiment; however, foaming problems existed at this concentrated of a cell density, and cell lysis may have contributed to the foaming problems (38). In a study for non-growing *S. cerevisiae* cells in an airlift probe, 40% v/v cell suspension could theoretically be supported under endogenous respiration using $k_l a$ calculations (55). However, only cell densities of up to 18% v/v could maintain of a cytoplasmic pH of 7.1-7.2 and a 0.2 pH unit difference over anaerobic conditions, thus indicating the utility of intracellular measurements in conjunction with engineering design calculations (55). Acquisitions times for a "good" ^{31}P NMR spectrum of cells in an airlift reactor are similar to those in an NMR bioassay.

Continuous Flow/Chemostat Reactors

In situ NMR studies of viable, actively growing cells has been especially challenging, but recent reports show promise. Sensitivity enhancement is possible for *in situ* samples (high T_1/ T_2*) if nuclear spins within the radiofrequency coil can be replaced by spins outside this region, thus shortening the time to acquire NMR spectra (4-6). A standard NMR sample tube was modified to study dilute (2 mg dw/ml) anaerobic bacteria in a continuous flow setup, with acquisition times for ^{31}P spectra under 0.5 hr (5). Significantly, the transmembrane pH gradient was larger for a dilute solution than a concentrated (123 mg dw/ml) density suspension (5). Aerobic systems have also been studied. An airlift reactor configuration in a previous study (38) was modified to a continuous flow system for a high cell density (23-27 mg dw/ml) culture of *E. coli* in late exponential phase (6). ^{31}P NMR spectra with acquisition times of under 14 minutes were obtained (6).

Aerobic, fairly low cell density (3-4% v/v) cultures of *S. cerevisiae* were successfully studied in a *in situ* NMR chemostat, with acquisition times for ^{31}P NMR spectra of under 7 minutes (7). The initial reactor construction, analysis of performance trade-offs, and a metabolic example are well described in a series of papers for this unique chemostat (4,7,56, 57). The discussion on reactor design and the tradeoffs that exist between net signal, spectral resolution, and oxygenation due to conductivity, sample volume, gas bubble and fluid flow effects is especially noteworthy (7). Although comparison of the acquisition times between the spectra from the *in situ* chemostat and the NMR bioassay at similar cell densities are not drastically different, the *in situ* chemostat has the distinct advantage of maintaining cells under controlled conditions for growth. These studies show significant promise for future metabolic studies. Additional work in characterizing the fraction of viable cells for accurate measurement in metabolite concentrations will be needed.

Future Directions

For the analysis of bioreactors, an NMR experimentalist's dream would be to place the entire bioreactor inside the magnet; to choose a plane or cube inside the bioreactor noninvasively; to photograph the configuration, measure the velocity, and detect several metabolites simultaneously on that volume; and then to have the option of taking several time points on several selected volume elements. A combination of NMR imaging and spectroscopy may be able to provide this data, and such technology is being investigated in medical research, where reactor flow becomes blood flow, and state variables become metabolic markers distinguishing disease from health.

However, until such technology is more readily available, subsets of these measurements can be performed on the current NMR systems. The analysis and configuration of the NMR reactor is steadily improving. Factors such as oxygenation, cell viability, mixing, mass transfer, and removal of toxic products upon NMR results continue to need to be addressed in the NMR system and in the application of these results to a larger reactor. The analysis of NMR data needs further exploration in terms of cellular metabolism. NMR results may conflict with those measured from other techniques. For example, differences observed in NMR versus extraction measurement of ADP concentrations may lead to a different interpretation of a bound versus free molecule in interaction with an enzyme or with multienzyme complexes. Further research on these issues are needed

so that the NMR can be exploited fully for its use as a biosensor. With further improvements in NMR technology, such as magnetic field strength and probe design, this goal is likely to be fulfilled.

Acknowledgements

Financial support from the National Science Foundation (BES-9213197), National Institute of Health (RR05759-01), and New Methods Research Inc. (NMR*i*) is gratefully acknowledged.

References

1. Lundberg, P., Harmsen, E., Ho, C. and Vogel, H. J. 1990. Nuclear magnetic resonance studies of cellular metabolism. Anal. Biochem. 191: 193-222.
2. Brindle, K. M. 1988. NMR methods for measuring enzyme kinetics *in vivo*. Prog. NMR Spec. 20: 257-293.
3. Gillies, R. J., Mackenzie, N. E. and Dale, B. E. 1989. Analyses of bioreactor performance by nuclear magnetic resonance spectroscopy. Bio/Technol. 7: 50-54.
4. Meehan, A. P., Eskey, C. J., Koretsky, A. P. and Domach, M. M. 1992. Cultivator for NMR studies of suspended cell cultures. Biotechnol. Bioeng. 40: 1359 - 1366.
5. De Graaf, A.A., Wittig, R. M., Probst, U., Strohhaecker, J., Schoberth, S. M., Sahm, H. 1992. Continuous-flow NMR bioreactor for *in vivo* studies of microbial cell suspensions with low biomass concentrations. J. Magn. Reson. 98: 654 – 659.
6. Chen, R., and Bailey, J. E. 1993. Observations of aerobic, growing *Escherichia coli* metabolism using an on-line nuclear magnetic resonance spectroscopy system. Biotechnol. Bioeng. 42: 215 - 221.
7. Castro, C.D., Koretsky, A. P. and Domach, M. M. 1999. Performance trade-offs in in situ chemostat NMR. Biotechnol. Prog. 15: 185 - 195.
8. Hoult, D. I. and Richards, R. E. 1976. The signal-to-noise ratio of the nuclear magnetic resonance experiments. J. Magn. Reson. 24: 71-85.
9. Burt, C. T., Cohen, S. M. and Barany, M. 1979. Analysis of intact tissue with ^{31}P NMR. Ann. Rev. Biophys. Bioeng. 8: 1-25.
10. den Hollander, J. A., Brown, T. R., Ugurbil, K. and Shulman, R. G. 1979. ^{13}C nuclear magnetic resonance studies of anaerobic glycolysis in suspensions of yeast cells. Proc. Natl. Acad. Sci. 76: 6096-6100.
11. den Hollander, J. A., Ugurbil, K., Brown, T. R. and Shulman, R. G. 1981. ^{31}P NMR resonance studies of the effect of oxygen upon glycolysis in yeast. Biochem. 20: 5871-5880.
12. Brindle, K., Williams, S.-P. and Boulton, M. 1989. ^{19}F NMR detection of a fluorine-labeled enzyme *in vivo*. Fed. Eur. Biochem. Soc. Let. 255: 121-124.
13. Gadian, D. G. 1982. Nuclear Magnetic Resonance and its Applications to Living Systems. New York, Oxford University Press.
14. Wray, S. and Tofts, P. S. 1986. Direct *in vivo* measurement of absolute concentrations using ^{31}P nuclear magnetic resonance spectroscopy. Biochim. Biophys. Acta. 886: 399-405.
15. Roos, A. and Boron, W. F. 1981. Intracellular pH. Physiol. Rev. 61: 296-434.
16. Roberts, J. K. M., Wade-Jardetzky, N. and Jardetzky, O. 1981. Intracellular pH measurements by ^{31}P nuclear magnetic resonance, influence of factors other than pH on ^{31}P chemical shifts. Biochem. 20: 5389-5394.
17. Shanks, J. V. and Bailey, J. E. 1988. Estimation of intracellular sugar phosphate concentrations in *Saccharomyces cerevisiae* using ^{31}P nuclear magnetic resonance spectroscopy. Biotechnol. Bioeng. 32: 1138-1152.
18. Gupta, R. K., Gupta, P. and Moore, R. D. 1984. NMR studies of intracellular metal ions in intact cells and tissues. Ann. Rev. Biophys. Bioeng. 13: 221-246.
19. Smith, G. A., Hesketh, R. T., Metcalfe, J. C., Feeney, J. and Morris, P. G. 1983. Intracellular calcium measurements by ^{19}F NMR of fluorine-labeled chelators. Proc. Natl. Acad. Sci. 80: 7178-7182.
20. Kanamori, K. and Roberts, J. D. 1983. ^{15}N NMR studies of biological systems. Acct. Chem. Res. 16: 35-41.
21. Lundberg, P., Weich, R. G., Jensen, P. and Vogel, H. J. 1989. Phosphorus-31 and nitrogen-14 NMR studies of the uptake of phosphorus and nitrogen compounds in the marine macroalgae *Ulva lactuca*. Plant Physiol. 89: 1380-1387.
22. Hofeler, H., Jensen, D., Pike, M. M., Delayre, J. L., Cirillo, V. P., Springer, C. S., Fossel, E. T. and Balschi, J. A. 1987. Sodium transport and phosphorus metabolism in sodium-loaded yeast: simultaneous observation with sodium-23 and phosphorus-31 NMR spectroscopy *in vivo*. Biochem. 26: 4953-4962.
23. Pan, J. W. and Macnab, R. M. 1990. Steady-state measurements of *Escherichia coli* sodium and proton potentials at alkaline pH support the hypothesis of electrogenic antiport. J. Biol. Chem. 265: 9247-9250.
24. Brindle, K. M., Braddock, P. and Fulton, S. 1990. ^{31}P NMR measurements of the ADP concentration in yeast cells genetically modified to express creatine kinase. Biochem. 29: 3295-3302.
25. Dijkema, C., De Vries, S. C., Booij, H., Schaafsma, T. J. and Van Kammen, A. 1988. Substrate utilization by suspension cultures and somatic embryos of *Daucus carota L.* measured by carbon-13 NMR. Plant Physiol. 88: 1332-1337.
26. Shanks, J. V. and Bailey, J. E. 1991. ^{31}P NMR and ^{13}C NMR studies of recombinant *Saccharomyces cerevisiae* with altered glucose phosphorylation activities. Bioproc. Eng. 6: 273-284.
27. Fernandez, E. J., Mancuso, A. and Clark, D. S. 1988. NMR spectroscopy studies of hybridoma metabolism in a simple membrane reactor. Biotechnol. Prog. 4: 173-183.
28. Schripsema, J., Erkelens, C. and Verpoorte, R. 1991. Intra- and extracellular carbohydrates in plant cell cultures investigated by proton-NMR. Plant Cell Rep. 9: 527-530.
29. Galazzo, J. L. and Bailey, J. E. 1989. *In vivo* nuclear magnetic resonance analysis of immobilization effects on glucose metabolism of yeast *Saccharomyces cerevisiae*. Biotechnol. Bioeng. 33: 1283-1289.
30. Galazzo, J. L., Shanks, J. V. and Bailey, J. E. 1990. Comparison of intracellular sugar-phosphate levels from ^{31}P nuclear magnetic resonance spectroscopy of intact cells and cell-free extracts. Biotechnol. Bioeng. 35: 1164 - 1168.
31. Galazzo, J. and Bailey, J. 1990. Fermentation pathway kinetics and metabolic flux control in suspended and immobilized *Saccharomyces cerevisiae*. Enzyme Microb. Technol. 12: 162-172.
32. Diaz-Ricci, J. C., Hitzmann, B. and Bailey, J. E. 1991. *In vivo* NMR analysis of the influence of pyruvate decarboxylase and alcohol dehydrogenase of *Zymomonas mobilis* on the anaerobic metabolism of *Escherichia coli*. Biotechnol. Prog. 7: 305-310.
33. Walker, T. E., Han, C. H., Kollman, V. H., London, R. E. and Matwiyoff, N. A. 1982. ^{13}C nuclear magnetic resonance studies of the biosynthesis by microbacterium ammoniaphilum of L-glutamate selectively enriched with carbon-13. J. Biol. Chem. 257: 1189-1195.
34. Walsh, K. and Koshland, D. E. 1984. Determination of flux through the branch point of two metabolic cycles. J. Biol. Chem. 259: 9646-9654.
35. Sumegi, B., Sherry, A. D. and Malloy, C. R. 1990. Channeling of TCA cycle intermediates in cultured *Saccharomyces cerevisiae*. Biochem. 29: 9106-9110.
36. Parhami, P. and Fung, B. M. 1983. ^{19}F relaxation study of perfluorochemicals as oxygen carriers. J. Phys. Chem. 87: 1928-1931.
37. Taylor, J. S. and Deutsch, C. J. 1987. Simultaneous measurement by NMR of O_2 tension and pH in cell suspensions. Biophys. J. 51: 77a.
38. Kramer, H. J. and Bailey, J. E. 1991. Mass transfer characterization of an airlift probe for oxygenating and mixing cell suspensions in an NMR spectrometer. Biotechnol. Bioeng. 37: 205-209.
39. Fernet, M.-D., Melvin, B., Gustin, M. and Shanks, J.V., 1994. ^{13}C NMR spectroscopy studies of glucose metabolism in osmolarity mutants of *Saccharomyces cerevisiae*, Enzyme Microb. Technol. 16: 207-215.
40. Bryers, J. D., Sayles, G. D. and Westcott, R. D. 1991. Posttranslational limitations to enzyme productivity in the methylotrophic yeast, *Hansenula polymorpha*. Chem. Eng. News. 69: 47.
41. Diaz-Ricci, J. C., Hitzmann, B., Rinas, U. and Bailey, J. E. 1990. Comparative studies of glucose catabolism by *Escherichia coli* grown in complex medium under aerobic and anaerobic conditions. Biotechnol. Prog. 6: 326-332.
42. Karel, S. F., Briasco, C. A. and Robertson, C. R. 1988. The behavior of immobilized living cells. Ann. N.Y. Acad. Sci. 84-105.
43. Karel, S. F. and Robertson, C. R. 1989. Cell mass synthesis and degradation by immobilized *Escherichia coli*. Biotechnol. Bioeng. 34: 337-356.
44. Drury, D. D., Dale, B. E. and Gillies, R. J. 1988. Oxygen transfer properties of a bioreactor for use within a nuclear magnetic resonance spectrometer. Biotechnol. Bioeng. 32: 966-974.
45. Fernandez, E. J., Mancuso, A., Murphy, M. K., Blanch, H. W. and Clark, D. S. 1990. Nuclear magnetic resonance methods for observing the intracellular environment of mammalian cells. Ann. N.Y. Acad. Sci. 589: 458-475.
46. Mancuso, A., Fernandez, E. J., Blanch, H. W. and Clark, D. S. 1990. A nuclear magnetic resonance technique for determining hybridoma

cell concentration in hollow fiber reactors. Bio/technol. 8: 1282-1285.
47. Fowler, J. D. and Robertson, C. R. 1990. Nutrient transport and cellular morphology in immobilized cell aggregates. Ann. N.Y. Acad. Sci. 589: 333-349.
48. Sharfstein, S. T., Tucker, S. N., Mancuso, A., Blanch, H. W., Clark, D. S. 1994. Quantitative *in vivo* nuclear magnetic resonance studies of hybridoma metabolism. Biotechnol. Bioeng. 43: 1059-1074.
49. Foxall, D. L. and Cohen, J. S. 1983. NMR studies of perfused cells. J. Magn. Res. 52: 346-349.
50. Brindle, K. and Krikler, S. 1985. ^{31}P-NMR saturation transfer measurements of phosphate consumption in *Saccharomyces cerevisiae*. Biochim. Biophys. Acta. 847: 285-292.
51. Barford, J. P. 1990. A general model for aerobic yeast growth: batch growth. Biotechnol. Bioeng. 35: 907-920.
52. Galazzo, J. L., Shanks, J. V. and Bailey, J. E. 1987. Comparison of suspended and immobilized yeast metabolism using ^{31}P nuclear magnetic resonance spectroscopy. Biotechnol. Techn. 1: 1-6.
53. Galazzo, J. L. and Bailey, J. E. 1990. Growing *Saccharomyces cerevisiae* in calcium-alginate beads induces cell alterations which accelerate glucose conversion to ethanol. Biotechnol. Bioeng. 36: 417-426.
54. Santos, H. and Turner, D. L. 1986. Characterization of the improved sensitivity obtained using a flow method for oxygenating and mixing cell suspensions in NMR. J. Magn. Reson. 68: 345-349.
55. Melvin, B.K. and Shanks, J.V., 1996. Influence of aeration on cytoplasmic pH of yeast in an NMR airlift reactor, Biotechnol. Prog. 12: 257-265.
56. Castro, C.D., Koretsky, A. P. and Domach, M. M. 1999. NMR-observed phosphate trafficking and polyphosphate dynamics in wild-type and vph1-1 mutant *Saccharomyces cerevisiae* in response to stresses. Biotechnol. Prog. 15: 65 - 73.
57. Castro, C.D., Meehan, A. J., Koretsky, A. P. and Domach, M. M. 1995. *In situ* ^{31}P NMR nuclear magnetic resonance for observation of polyphosphate and catabolite responses of chemostat-cultivated *Saccharomyces cerevisiae* after alkalinization. Appl. Environ. Microbiol. 61: 4448 - 4453.

Further Reading

Caister Academic Press is a leading academic publisher of advanced texts in microbiology, molecular biology and medical research. Full details of all our publications at **caister.com**

- **MALDI-TOF Mass Spectrometry in Microbiology**
  Edited by: M Kostrzewa, S Schubert (2016)
  www.caister.com/malditof
- ***Aspergillus* and *Penicillium* in the Post-genomic Era**
  Edited by: RP Vries, IB Gelber, MR Andersen (2016)
  www.caister.com/aspergillus2
- **The Bacteriocins: Current Knowledge and Future Prospects**
  Edited by: RL Dorit, SM Roy, MA Riley (2016)
  www.caister.com/bacteriocins
- **Omics in Plant Disease Resistance**
  Edited by: V Bhadauria (2016)
  www.caister.com/opdr
- **Acidophiles: Life in Extremely Acidic Environments**
  Edited by: R Quatrini, DB Johnson (2016)
  www.caister.com/acidophiles
- **Climate Change and Microbial Ecology: Current Research and Future Trends**
  Edited by: J Marxsen (2016)
  www.caister.com/climate
- **Biofilms in Bioremediation: Current Research and Emerging Technologies**
  Edited by: G Lear (2016)
  www.caister.com/biorem
- **Microalgae: Current Research and Applications**
  Edited by: MN Tsaloglou (2016)
  www.caister.com/microalgae
- **Gas Plasma Sterilization in Microbiology: Theory, Applications, Pitfalls and New Perspectives**
  Edited by: H Shintani, A Sakudo (2016)
  www.caister.com/gasplasma
- **Virus Evolution: Current Research and Future Directions**
  Edited by: SC Weaver, M Denison, M Roossinck, et al. (2016)
  www.caister.com/virusevol
- **Arboviruses: Molecular Biology, Evolution and Control**
  Edited by: N Vasilakis, DJ Gubler (2016)
  www.caister.com/arbo
- ***Shigella*: Molecular and Cellular Biology**
  Edited by: WD Picking, WL Picking (2016)
  www.caister.com/shigella
- **Aquatic Biofilms: Ecology, Water Quality and Wastewater Treatment**
  Edited by: AM Romaní, H Guasch, MD Balaguer (2016)
  www.caister.com/aquaticbiofilms
- **Alphaviruses: Current Biology**
  Edited by: S Mahalingam, L Herrero, B Herring (2016)
  www.caister.com/alpha
- **Thermophilic Microorganisms**
  Edited by: F Li (2015)
  www.caister.com/thermophile

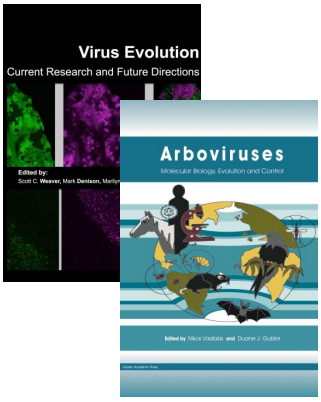

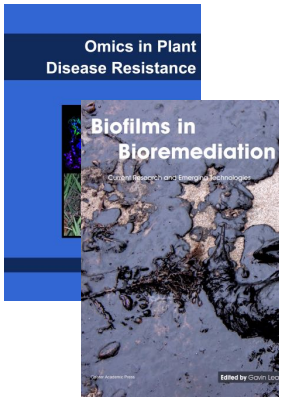

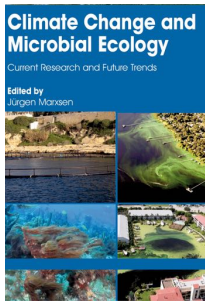

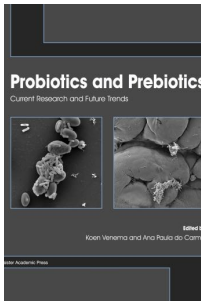

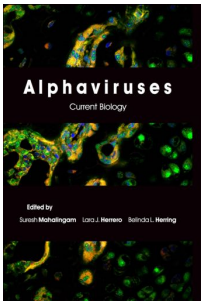

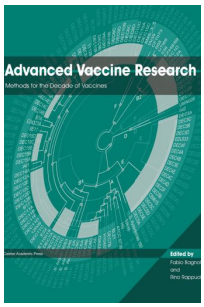

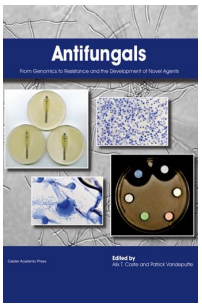

- **Flow Cytometry in Microbiology: Technology and Applications**
  Edited by: MG Wilkinson (2015)
  www.caister.com/flow
- **Probiotics and Prebiotics: Current Research and Future Trends**
  Edited by: K Venema, AP Carmo (2015)
  www.caister.com/probiotics
- **Epigenetics: Current Research and Emerging Trends**
  Edited by: BP Chadwick (2015)
  www.caister.com/epigenetics2015
- ***Corynebacterium glutamicum*: From Systems Biology to Biotechnological Applications**
  Edited by: A Burkovski (2015)
  www.caister.com/cory2
- **Advanced Vaccine Research Methods for the Decade of Vaccines**
  Edited by: F Bagnoli, R Rappuoli (2015)
  www.caister.com/vaccines
- **Antifungals: From Genomics to Resistance and the Development of Novel Agents**
  Edited by: AT Coste, P Vandeputte (2015)
  www.caister.com/antifungals
- **Bacteria-Plant Interactions: Advanced Research and Future Trends**
  Edited by: J Murillo, BA Vinatzer, RW Jackson, et al. (2015)
  www.caister.com/bacteria-plant
- ***Aeromonas***
  Edited by: J Graf (2015)
  www.caister.com/aeromonas
- **Antibiotics: Current Innovations and Future Trends**
  Edited by: S Sánchez, AL Demain (2015)
  www.caister.com/antibiotics
- ***Leishmania*: Current Biology and Control**
  Edited by: S Adak, R Datta (2015)
  www.caister.com/leish2
- ***Acanthamoeba*: Biology and Pathogenesis (2nd edition)**
  Author: NA Khan (2015)
  www.caister.com/acanthamoeba2
- **Microarrays: Current Technology, Innovations and Applications**
  Edited by: Z He (2014)
  www.caister.com/microarrays2
- **Metagenomics of the Microbial Nitrogen Cycle: Theory, Methods and Applications**
  Edited by: D Marco (2014)
  www.caister.com/n2

Order from caister.com/order